Solar-Terrestrial Physics, 2017. Vol. 3. Iss. 2, pp. 60–64, DOI: 10.12737/stp-32201710. © INFRA-M Academic Publishing House
Original Russian version Jing Jiao, Guotao Yang, Jihong Wang, Xuewu Cheng, Faqun Li,
published in Solnechno-Zemnaya Fizika, 2017, vol. 3, iss. 2, pp. 64–69, DOI: 10.12737/22597

SPORADIC POTASSIUM LAYERS AND THEIR CONNECTION TO SPORADIC E LAYERS IN THE MESOPAUSE REGION AT BEIJING, CHINA

Jing Jiao
State Key Laboratory of Space Weather, National Space Science Center, Chinese Academy of Sciences, Beijing, China, jjiao@spaceweather.ac.cn
China-Brazil Joint Laboratory for Space Weather, Chinese Academy of Sciences, 8 São Jose dos Campos, Brazil

Guotao Yang
State Key Laboratory of Space Weather, National Space Science Center, Chinese Academy of Sciences, Beijing, China

Jihong Wang
State Key Laboratory of Space Weather, National Space Science Center, Chinese Academy of Sciences, Beijing, China

Xuewu Cheng
Wuhan Institute of Physics and Mathematics, Chinese Academy of Sciences, Wuhan, China

Faqun Li
Wuhan Institute of Physics and Mathematics, Chinese Academy of Sciences, Wuhan, China

Abstract. A double-laser beam lidar to measure potassium (K) layer at Beijing (40.5° N, 116.2° E) was successfully developed in 2010. The parameters of sporadic K_s layers and their distributions were given. The seasonal distribution of K_s occurrence frequency was obtained, with two maxima in July and January. The seasonal distributions of sporadic E_s layer occurrence frequency over Beijing differ from those of K_s. However, the good correlation between E_s and K_s in the case-by-case studies supports the mechanism of neutralization of metal ions in a descending E_s layer.

Keywords: lidar, sporadic potassium layers, sporadic E layers.

1. INTRODUCTION

Meteoric metal (Na, K, Ca, Mg, etc.) layers between 80 and 110 km originate from meteor ablation [Plane, 1991; Kane et al., 2001]. Lidar observations and studies of metal layers have been carried out for about 40 years, promoting better understanding of chemical and dynamic processes in the mesopause region. Sporadic or narrow metal layers (N_s) were often observed in lidar data.

There are fewer lidar observations of the K layer than the sodium (Na) one. This is because the density of the K layer is approximately two orders of magnitude lower than that of the Na layer [Megie et al., 1978]. While several lidar observations of K layers over different regions were made [Eska, Hoffner, 1988; Eska et al., 1998; von Zahn et al., 1999; Friedman et al., 2002], reports on K_s layers were limited in number: two different sporadic layer events were analyzed by Delgado et al. [2012], and the K_s layers were observed in both neutral K and Ca^+ layers with a lidar. A temperature-dependent chemical model was also developed to simulate the observations: one event that occurred between June 12 and 13, 2002 was successfully reproduced. Raizada et al. [2004] found that sudden increases in both K and Ca densities were often observed during early morning hours or at night when meteor showers occurred.

Among many mechanisms for interpreting the N_s formation, the most promising is the neutralization of ions, as evidenced by the high temporal and spatial correlation between enhanced metal atoms and E_s layers [Gardner et al., 1993; Friedman et al., 2000; Williams et al., 2007; Delgado et al., 2012; Dou et al., 2012]. However, no reports examined the relationship between the K_s and E_s layers.

In this paper, using lidar and digital ionosonde observations from the newly launched Meridian Project, the aim of which is to help researchers better understand and predict space weather conditions over China, we statistically analyzed the K_s and E_s layer events at Beijing. The observational data were obtained by the Na-K lidar at Beijing from November 2010 to October 2011 and from May 2013 to April 2014.

2. DEVICES AND METHODS

2.1. Na-K lidar

Our double-laser-beam lidar for K and Na layer measurements is an upgrade of the Beijing LIDAR used in the Chinese Meridian Project [Wang, 2010]. Figure 1 is the schematic of the lidar system. A twice secondary harmonic generation technique [Cheng et al., 2011] has been used. A pulsed Nd:YAG laser outputs a 1064 nm beam, which is sent into a frequency multiplier to produce a 532 nm laser beam. The remainder of the 1064 nm laser beam is sent into another frequency multiplier again, and thus we get two 532 nm laser beams. These

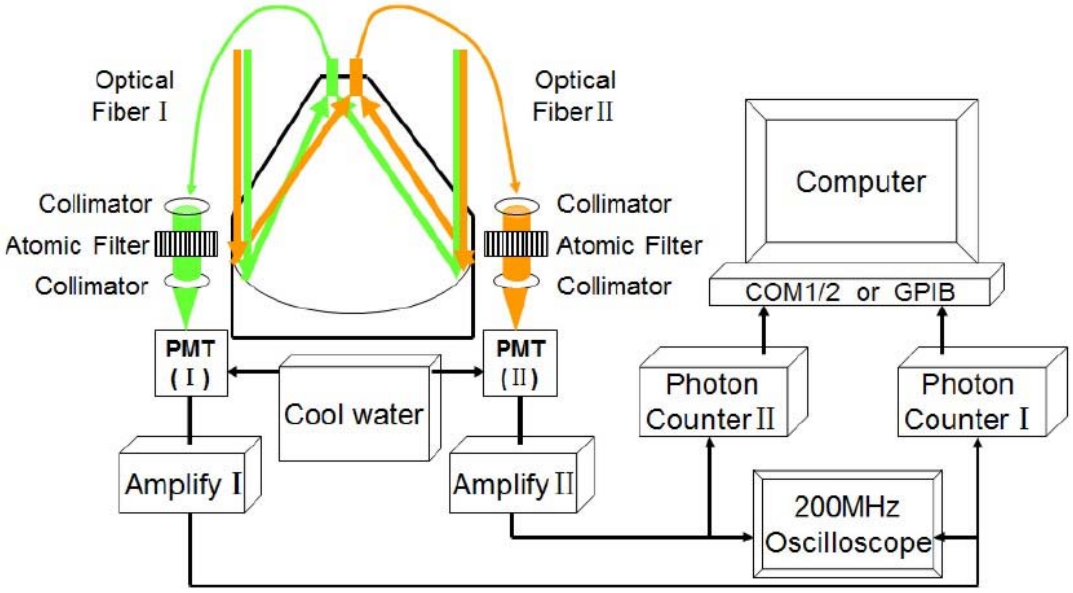

Figure 1. Lidar system

two 532 nm laser beams are used to pump two dye lasers. A 589 nm laser beam is then produced to detect Na atoms, and a 770 nm laser beam is produced to detect K atoms. The repetition rate of the Nd:YAG laser is 30 Hz. The output energy of the 589 nm laser beam is 40 mJ per pulse, while for the 770 nm laser beam the output is 60 mJ. Backscattered fluorescence photons from the Na and K layers are detected by a Cassegrain telescope with a 100 cm diameter primary mirror.

Signals from 10000 laser pulses are integrated to produce a K layer profile (for a corresponding temporal resolution of 5.5 min); 5000 laser pulses are used for a Na profile (for a corresponding temporal resolution of 2.8 min). To increase the signal-to-noise ratio (SNR) in the K-layer data, a five point average in height is used in the analysis. The configuration of the lidar system is summarized in Table.

This Na-K lidar system was operated from November 2010 to October 2011 and from May 2013 to April 2014; about 2000 hr (209 nights) of data were collected with fairly good SNR (the background noise was generally no more than 250). The absolute densities of K atoms were obtained by using a standard inversion procedure and by considering the back-scattered cross section of K (D1) transitions, as well as the laser bandwidth.

The K_s layer events were selected according to the following criteria: (1) the maximum density of the K_s peak must be at least three times higher than that of the normal K layer at the same altitude (i.e., a strength factor≥3); (2) the maximum density of the K_s peak must be more than 1/2 of the peak density of the normal K layer (because at high altitude, K_s events can be associated with a larger strength factor and a very low relative density); (3) the full-width-at-half-maximum (FWHM) of the K_s layer must be <3 km; and (4) the K_s event must last for at least three successive lidar profiles. These criteria are similar to those described by Gong et al. [2002].

Main Specifications of the Na-K Lidar System

	Na	K
Transmitter:		
Wavelength, nm	589	770
Pulse energy, mJ	40	60
Line width, GHz	1.5	1.5
Pulse width, ns	~10	~10
Repetition rate, Hz	30	30
Beam divergence, mrad	<0.5	<0.5
Receiver telescope		
Type	Cassegrain	
Diameter, mm	~Φ1000	~Φ1000
Field of view, mrad	2	2
Receiver filter		
Wavelength, nm	589	770
Bandwidth, nm	1	1

2.2. Digital ionosonde equipment

Digital ionosonde equipment was also employed to study the correlation of sporadic Na_s layer with sporadic E_s layer. Our digital ionosonde which also belongs to the Meridian Project is located ~24 km southeast of the lidar site in the Changping District (Beijing). In this configuration, the lidar and the ionosonde detect nearly a common volume in the mesopause region. The ionosonde records data automatically every 15 min, and its frequency scans from 0.5 to 15 MHz in 150 s to form a data file. For comparison, we chose data collected from November 2010 to October 2011 and from May 2013 to April 2014 at Beijing, which were obtained by both the ionosonde and the lidar. Reading the ionosonde SAO files makes the E_s-layer parameters available, such as its f_oE_s (the critical frequency) and $h'E_s$ (the virtual height).

3. RESULTS

An example of the contour plot and the single profile at the moment when K_s reached its maximum density at Beijing on May 29, 2013 are shown in Figure 2. As can be seen in Figure 2, *a*, the K_s appeared at 22:18 LT and then disappeared at 22:43 LT. Thus, the duration of the K_s event was about 1 h. From the profile at its maximum at 23:09 LT (Figure 2, *b*), we can obtain its general properties. For example, the peak K density of K_s is 161.25 cm^{-3}, the relevant altitude is 102.62 km, the FWHM is 0.29 km, and the strength factor is 6.83.

The seasonal distribution of K_s occurrence at our location is shown in Figure 3, *a*. We noticed that the K_s occurrence under study was not smoothly distributed over the year. As shown in the Figure, the K_s occurrence has maximum value in January and July. The seasonal distribution of E_s occurrence at our location is illustrated in Figure 3, *b*. Here, the digital ionosonde data are used for the analysis. We noticed that, unlike the K_s events, the E_s occurrence is smoothly distributed over the months of the year. The E_s occurrence has maximum value in May, and the E_s occurrence in the summer months is much higher than that in other seasons. In February, the E_s occurrence is the lowest. From these observations it was evident that K_s and E_s occurrences are characterized by completely different seasonal variations.

The K_s and E_s events were also compared on a case-by-case basis. Owing to the limited number of ionosonde data, we could compare only 21 of the 58 K_s events. We observed that 15 of the 21 events verified that K_s events corresponded with E_s events. A histogram comparing the time differences for the 15 pairs of events is given in Figure 4. In the previous study of Na_s layers, researchers frequently compared the time of occurrence of Na_s and E_s layers to prove the mechanism

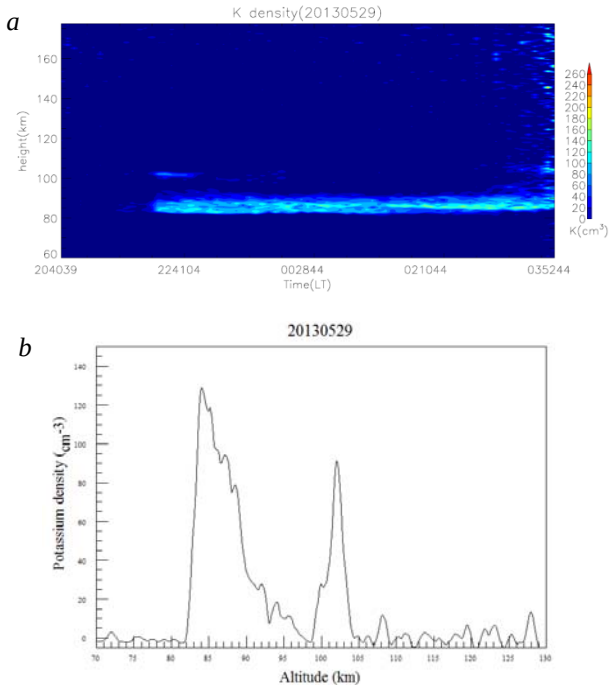

Figure 2. Contour of the K layer observed at the Beijing site from 20:40:39 LT on May 29, 2013 to 03:52:44 LT on May 30, 2013 (*a*); the K density profile observed at 23:16 LT (*b*)

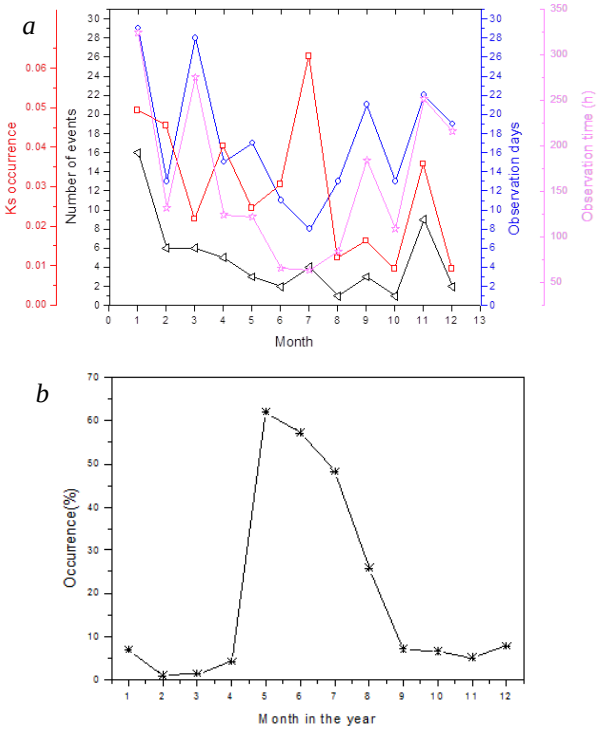

Figure 3. Seasonal distributions of K_s occurrence (frequency and numbers) at our location and the observation time (days and hours) in each month (*a*); seasonal distribution of E_s occurrence (*b*)

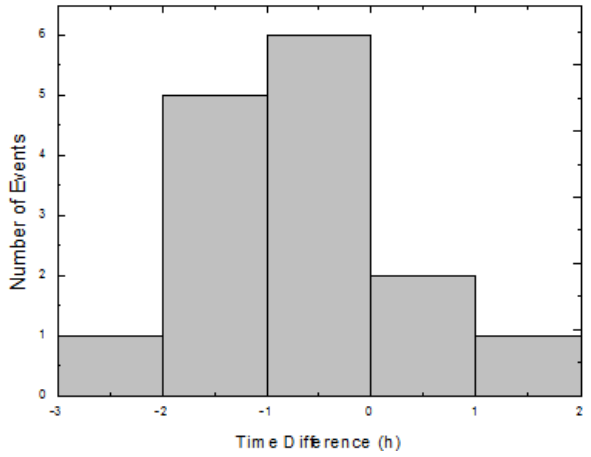

Figure 4. Distribution of the time difference between K_s and E_s (the negative value represents E_s reaching its lowest height before K_s reaches its maximum)

by which Na^+ in the E_s layer was neutralized to Na [Gong et al., 2002]. As deduced from the previous observation of the Na_s layers, when E_s descended to the lowest height with time, the Na density reached its maximum [Gong et al., 2002; Ma et al., 2014]. Therefore, we defined the time difference between K_s and E_s in a similar way: the time difference refers to the time when a K_s event developed to its maximum intensity and an E_s event to its minimum height, with the negative values representing E_s reaching its minimum height before K_s reaches its maximum intensity. As shown in the Figure, all 15 associated E_s events reached their minimum heights within 3 h before and 2 h after, with a

mean value of less than 1 h before the corresponding K_s events reached their maximum intensities.

4. DISCUSSION

The seasonal distribution of K_s occurrence frequency is also quite different with that of E_s. The maximum of E_s occurrence frequency is observed in summer and the minimum in winter. These results are much different with those of K_s, as many K_s events were observed in winter. However, a relative good relationship between K_s and E_s was found in the case-by-case study. So we need to consider the most accepted mechanism by which metal ions are neutralized to form atoms in a descending E layer.

The height distribution of E_s in different seasons is shown in Figure 5. The Y axis represents the lowest E_s height in the observation night; the black circle marks different E_s heights for different days, and the red line represents the fitted curve of the distribution. The distribution of E_s heights presents a semiannual variation with minima in winter and summer, and the K_s occurrence has two maxima in winter and summer, as seen from Figure 3, *a*. Due to the lower height of the winter E_s, the K ion is more easily converted into K_s, but the E_s occurrence is lower in winter, because the E_s layers have different contents of Na and K elements.

Neutralization of K^+ occurs by forming a cluster ion with a ligand X, where X=N_2, O_2, O (in order of decreasing concentration in mesopause and lower thermosphere (MLT) region) [Eska et al., 1999]. The recombination is shown as follows:

$$K^+ + X(+M) \rightleftharpoons K^+X \quad (1)$$

$$K^+X + Y \rightleftharpoons K^+Y + X \quad (2)$$

$$K^+(X_{or}Y) + e^- \rightleftharpoons K + X_{or}Y \quad (3)$$

where M is the third body (most likely N_2 or O_2). K^+ is a relatively large singly-charged ion (cf. Na^+). It forms very weakly bound clusters with the major species (N_2, O_2, and O) in MLT, with binding energies less than 20 kJ/mol. Therefore, the sequence of reactions (1)–(3) becomes significant at very low temperatures characteristic of summertime MLT [Plane et al., 2014].

Ernest Kopp pointed out that Na ions in the ionosphere are about ten times of K ions [Kopp, 1997]. Although Na ions are about a few hundreds, it is difficult to produce Na_s. Although the K ion density is only about a few dozen per cubic centimeter, K density is also only about a few dozen per cubic centimeter, so that K ions are more prone to produce K_s. So, compared to other months, the E_s layer contains more K ions in January. Furthermore, it is easier to produce K_s events through ion–neutral reactions.

5. CONCLUSION

Of two years of lidar observations, 58 K_s events are observed in 2000 hr of data. Seasonal distributions of K_s occurrence were obtained, with two maxima found in July and January. Many K_s events occurred in November, January, and February (especially in January).

The relation between K_s and E_s was analyzed. The K_s and E_s occurrences have different seasonal variations. The K_s occurrence has a maximum in July and a secondary maximum in January, but the E_s occurrence has a minimum value in winter. The probable reason for the high occurrence of K_s in January is that it is easier to produce K_s events through ion–neutral reactions, considering that the E_s layer contains relatively more K ions in January. However, the relatively good relation between K_s and E_s was found in the case-by-case study. The K ion is more easily converted into K_s because E_s heights are relatively low in winter. So, we need to consider the most accepted mechanism by which that metal ions are neutralized to form atoms in the descending E

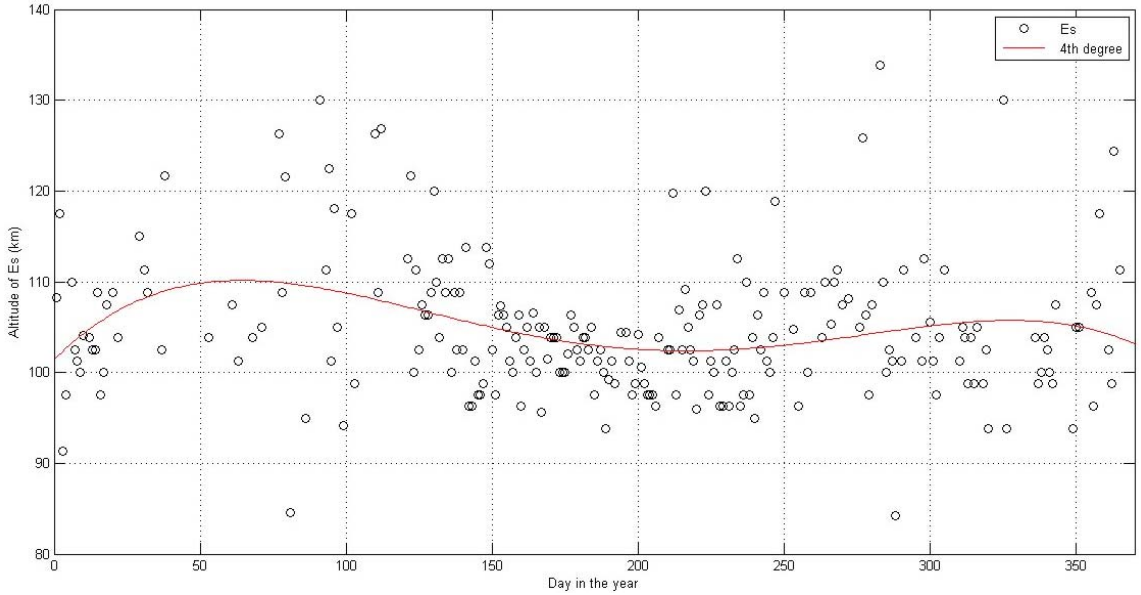

Figure 5. Height distribution of E_s events in the year. The black circle represents different E_s heights for different days; the red line marks the fitted curve of the distribution

layer. As a consequence, more combined observations are needed to develop further understanding of the K_s formation mechanism.

We acknowledge the use of the data from the Chinese Meridian Project (http://www.meridianproject.ac.cn/). The work was supported by the Natural Science foundation of China (the grants No. 41474130, 41264006), NSSC research fund for key development directions, the Specialized Research Fund for State Key Laboratories of China, and China-Brazil Joint Laboratory for Space Weather, CAS.

REFERENCES

Cheng X., Yang G., Yang Y., Li F., Wang J., Liu Y., Li Y., Lin X., Gong S. Na layer and K layer simultaneous observation by lidar. *Chinese J. Lasers*. 2011, vol. 38, no. 2, pp. 233–237. (In Chinese).

Delgado R., Friedman J.S., Fentzke J.T., Raizada S., Tepley C.A., Zhou Q. Sporadic metal atom and ion layers and their connection to chemistry and thermal structure in the mesopause region at Arecibo. *J. Atmos. Solar-Terr. Phys*. 2012, vol. 74, pp. 11–23. DOI: 10.1016/j.jastp.2011.09.004.

Dou X.K., Xue X.H., Li T., Chen T.D., Chen C., Qiu S.C. Possible relations between meteors, enhanced electron density layers, and sporadic sodium layers. *J. Geophys. Res.: Space Phys.* 2010, vol. 115., CiteID A06311. DOI: 10.1029/2009ja014575.

Eska V., Hoffner J. Observed linear and nonlinear K layer response. *Geophys. Res. Lett.* 1998, vol. 25, no. 15, pp. 2933–2936. DOI: 10.1029/98gl02110.

Eska V., Hoffner J., von Zahn U. Upper atmosphere potassium layer and its seasonal variations at 54 degrees N. *J. Geophys. Res.: Space Phys.* 1998, vol. 103, no. A12, pp. 29207–29214. DOI: 10.1029/98ja02481.

Eska V., von Zahn U., Plane J.M.C. The terrestrial potassium layer (75–110 km) between 71 degrees S and 54 degrees N: Observations and modeling, *J. Geophys. Res.: Space Phys.* 1999, vol. 104, no. A8, pp. 17173–17186. DOI: 10.1029/1999ja900117.

Friedman J.S., Collins S.C., Delgado R., Castleberg P. A. Mesospheric potassium layer over the Arecibo Observatory, 18.3 degrees N 66.75 degrees W. *Geophys. Res. Lett.* 2002, vol. 29, no. 5, pp. 15-1, CiteID 1071. DOI: 10.1029/2001gl013542.

Friedman J.S., Gonzalez S.A., Tepley C.A., Zhou Q., Sulzer M.P., Collins S.C., Grime B.W. Simultaneous atomic and ion layer enhancements observed in the mesopause region over Arecibo during the Coqui II sounding rocket campaign. *Geophys. Res. Lett*. 2000, vol. 27, no. 4, pp. 449–452. DOI: 10.1029/1999gl900605.

Gardner C.S., Kane T.J., Senft D.C., Qian J., Papen G.C. Simultaneous observations of sporadic-E, Na, Fe, and Ca+ layers at Urbana, Illinois – 3 case-studies. *J. Geophys. Res.: Atmos.* 1993, vol. 98, no. D9, pp. 16865–16873. DOI: 10.1029/93jd01477.

Gong S.S., Yang G.T., Wang J.M., Liu B.M., Cheng X.W., Xu J.Y., Wan W.X. Occurrence and characteristics of sporadic sodium layer observed by lidar at a mid-latitude location. *J. Atmos. Solar-Terr. Phys.* 2002, vol. 64, no. 18, pp. 1957–1966. DOI: http://dx.doi.org/10.1016/S1364-6826(02)00216-X.

Kane T., Grime B., Franke S., Kudeki E., Urbina J., Kelley M., Collins S. Joint observations of sodium enhancements and field-aligned ionospheric irregularities *Geophys. Res. Lett.* 2001, vol. 28, no. 7, pp. 1375–1378. DOI: 10.1029/2000gl012176.

Ma Z., Wang X., Chen L., Wu J. First report of sporadic Na layers at Qingdao (36 degrees N, 120 degrees E), China. *Ann. Geophys.* 2014, vol. 32, no. 7, pp. 739–748. DOI: 10.5194/angeo-32-739-2014.

Megie G., Bos F., Blamont J.E., Chanin M.L. Simultaneous nighttime lidar measurements of atmospheric sodium and potassium. *Planetary and Space Sci.* 1978, vol. 26, no. 1, pp. 27–35. DOI: 10.1016/0032-0633(78)90034-x.

Plane J.M.C. The chemistry of meteoric metals in the Earth's upper-atmosphere. *Int. Rev. Phys. Chem.* 1991, vol. 10, no. 1, pp. 55–106. DOI: 10.1080/01442359109353254.

Plane J.M.C., Feng W., Dawkins E., Chipperfield M.P., Höffner J., Janches D., Marsh D.R. Resolving the strange behavior of extraterrestrial potassium in the upper atmosphere. *Geophys. Res. Lett.* 2014, vol. 41, no. 13, pp. 4753–4760. DOI: 10.1002/2014GL060334.

Raizada S., Tepley C.A., Janches D., Friedman J.S., Zhou Q., Mathews J.D. Lidar observations of Ca and K metallic layers from Arecibo and comparison with micrometeor sporadic activity. *J. Atmos. Solar-Terr. Phys.* 2004, vol. 66, no. 6–9, pp. 595–606. DOI: http://dx.doi.org/10.1016/ j.jastp.2004.01.030.

von Zahn U., Gerding M., Hoffner J., McNeil W.J., Murad E. Iron, calcium, and potassium atom densities in the trails of Leonids and other meteors: Strong evidence for differential ablation. *Meteoritics & Planetary Sci.* 1999, vol. 34, no. 6, pp. 1017–1027.

Wang C. New chains of space weather monitoring stations in China. *Space Weather*. 2010, vol. 8, no. 8, S08001. DOI: 10.1029/2010SW000603.

Williams B.P., Berkey F.T., Sherman J., She C.Y. Coincident extremely large sporadic sodium and sporadic E layers observed in the lower thermosphere over Colorado and Utah. *Ann. Geophys*. 2007, vol. 25, no. 1, pp. 3–8.

How to cite this article

Jing Jiao, Guotao Yang, Jihong Wang, Xuewu Cheng, Faqun Li. Sporadic potassium layers and their connection to sporadic E layers in the mesopause region at Beijing, China. Solar-Terr. Phys. 2017. Vol. 3. Iss. 2. P. 60–64.